JPET Fast Forward. Published on January 11, 2023 as DOI: 10.1124/jpet.122.001393
This article has not been copyedited and formatted. The final version may differ from this version.

Title Page:

Initial pharmacological characterization of a major hydroxy metabolite of PF-5190457: inverse agonist activity of PF-6870961 at the ghrelin receptor

Sara L. Deschaine[1,2], Morten A. Hedegaard[3], Claire L. Pince[1,4], Mehdi Farokhnia[1,5], Jacob E. Moose[6], Ingrid A. Stock[7], Sravani Adusumalli[8], Fatemeh Akhlaghi[8], James L. Hougland[6,9,10], Agnieszka Sulima[11,12], Kenner C. Rice[11,12], George F. Koob[4], Leandro F. Vendruscolo[4], Birgitte Holst[3], Lorenzo Leggio[1,11,13,14]*

1. Clinical Psychoneuroendocrinology and Neuropsychopharmacology Section, Translational Addiction Medicine Branch, National Institute on Drug Abuse Intramural Research Program and National Institute on Alcohol Abuse and Alcoholism Division of Intramural Clinical and Biological Research, National Institutes of Health, Baltimore and Bethesda, MD, USA
2. Department of Pharmacology, University of Michigan Medical School, Ann Arbor, MI, USA
3. Department of Biomedical Sciences, University of Copenhagen, Denmark
4. Neurobiology of Addiction Section, Integrative Neuroscience Research Branch, National Institute on Drug Abuse, National Institutes of Health, Baltimore, MD, USA
5. Department of Mental Health, Johns Hopkins Bloomberg School of Public Health, Johns Hopkins University, Baltimore, MD, USA
6. Department of Chemistry, Syracuse University, Syracuse, NY, USA
7. Pfizer Inc. Medicine Design, Eastern Point Road, Groton, CT, USA
8. Clinical Pharmacokinetics Research Laboratory, Department of Biomedical and Pharmaceutical Sciences, University of Rhode Island, Kingston, RI, USA
9. Department of Biology, Syracuse University, Syracuse, NY, USA
10. BioInspired Syracuse, Syracuse University, Syracuse, NY, USA
11. Medication Development Program, National Institute on Drug Abuse Intramural Research Program, National Institutes of Health, Baltimore, MD, USA

12. Drug Design and Synthesis Section, Molecular Targets and Medications Discovery Branch, Intramural Research Program, National Institute on Drug Abuse and National Institute on Alcohol Abuse and Alcoholism, National Institutes of Health, Bethesda MD, USA
13. Center for Alcohol Addiction Studies, Department of Behavioral and Social Sciences, School of Public Health, Brown University, Providence, RI, USA
14. Division of Addiction Medicine, Department of Medicine, School of Medicine, Johns Hopkins University, Baltimore, MD, USA

***Corresponding author:**

Lorenzo Leggio, M.D., Ph.D.

NIDA and NIAAA, National Institutes of Health

251 Bayview Boulevard, Biomedical Research Center, Room 04A511, Baltimore, MD 21224

Emails: lorenzo.leggio@nih.gov

JPET Fast Forward. Published on January 11, 2023 as DOI: 10.1124/jpet.122.001393
This article has not been copyedited and formatted. The final version may differ from this version.

Running Title Page:

Running Title: PF-5190457 metabolite activity at the ghrelin receptor

Word Count (Abstract, Introduction, Discussion): 2,829

Manuscript Pages: 31

Total Figures: 7

Total Tables: 4

JPET Fast Forward. Published on January 11, 2023 as DOI: 10.1124/jpet.122.001393
This article has not been copyedited and formatted. The final version may differ from this version.

Abstract:

Preclinical and clinical studies have identified the ghrelin receptor (growth hormone secretagogue receptor 1a; GHSR1a) as a potential target for treating alcohol use disorder. A recent Phase 1a clinical trial of a GHSR1a antagonist/inverse agonist, PF-5190457, in individuals with heavy alcohol drinking, identified a previously undetected major hydroxy metabolite of PF-5190457, namely PF-6870961. Here, we further characterized PF-6870961 by screening for off-target interactions in a high throughput screen and determined its *in vitro* pharmacodynamic profile at GHSR1a through binding and concentration-response assays. Moreover, we determined whether the metabolite demonstrated an *in vivo* effect by assessing effects on food intake in male and female rats. We found that PF-6870961 had no off-target interactions and demonstrated both binding affinity and inverse agonist activity at GHSR1a. In comparison to its parent compound, PF-5190457, the metabolite PF-6870961 had lower binding affinity and potency at inhibiting GHSR1a-induced inositol phosphate accumulation. However, PF-6870961 had increased inhibitory potency at GHSR1a-induced β-arrestin recruitment relative to its parent compound. Intraperitoneal injection of PF-6870961 suppressed food intake under conditions of both food restriction and with *ad libitum* access to food in male and female rats, demonstrating *in vivo* activity. The effects of PF-6870961 on food intake were abolished in male and female rats knock-out for GHSR, thus demonstrating that its effects on food intake are in fact mediated by the GHSR receptor. Our findings indicate that the newly discovered major hydroxy metabolite of PF-5190457 may contribute to the overall activity of PF-5190457 by demonstrating inhibitory activity at GHSR1a.

Significance statement: Antagonists or inverse agonists of the growth hormone secretagogue receptor (GHSR1a) have demonstrated substantial potential as therapeutics for alcohol use disorder. We here expand understanding of the pharmacology of one such GHSR1a inverse agonist, PF-5190457, by studying the safety and pharmacodynamics of its major hydroxy metabolite, PF-6870961. Our data demonstrate biased inverse agonism of PF-6870961 at GHSR1a and provides new structure-activity relationship insight into GHSR1a inverse agonism.

JPET Fast Forward. Published on January 11, 2023 as DOI: 10.1124/jpet.122.001393
This article has not been copyedited and formatted. The final version may differ from this version.

1. Introduction

Alcohol use disorder (AUD) is a chronic relapsing disease that causes significant harm to an individual's health and is a growing public health concern. However, the number of medications approved to treat AUD remains low, leaving critical need for a broader range of AUD therapeutics. Growing evidence indicates a role of the stomach-derived peptide ghrelin in AUD. Ghrelin, acylated by ghrelin O-acyl transferase (GOAT) to obtain receptor activity, plays important roles in nutrient sensing and informs homeostatic and hedonic processes regulating appetitive behaviors, including alcohol consummatory behaviors (for reviews, see (Yanagi, Sato et al. 2018, Deschaine and Leggio 2022)). This role is evidenced by preclinical and clinical studies demonstrating that ghrelin potentiates alcohol seeking and craving (for reviews, see (Morris, Voon et al. 2018, Farokhnia, Faulkner et al. 2019)). In rodents, ghrelin increases alcohol self-administration, alcohol-induced conditioned place preference, and alcohol-induced dopamine release in the nucleus accumbens (Jerlhag, Egecioglu et al. 2009). Moreover, antagonism or knockout of the ghrelin receptor (growth hormone secretagogue receptor 1a; GHSR1a) decreases alcohol self-administration (Kaur and Ryabinin 2010, Landgren, Simms et al. 2012, Suchankova, Steensland et al. 2013, Morris, Voon et al. 2018, Yanagi, Sato et al. 2018, Zallar, Beurmann et al. 2019, Zallar, Beurmann et al. 2019a). In humans, intravenous (IV) administration of ghrelin increases self-reported alcohol craving (Leggio, Zywiak et al. 2014), alcohol self-administration, and functional magnetic resonance imaging (fMRI) blood oxygen level dependent (BOLD) reactivity to alcohol symbols in the amygdala (Farokhnia, Grodin et al. 2018). Thus, inhibiting the activity of the ghrelin system has been suggested as a potential pharmacotherapy for AUD, which may extend to other substance use disorders as well (for review, see (Zallar, Farokhnia et al. 2017) (You, Galaj et al. 2022).

The effects of ghrelin on alcohol-related behaviors occur through interaction with its receptor, GHSR1a. GHSR1a is a G-protein coupled receptor (GPCR) expressed both centrally and peripherally that demonstrates ligand-independent, constitutive activity (Holst, Cygankiewicz et al. 2003) and couples to $G\alpha_q$, $G\alpha_{12/13}$, $G\alpha_{i/o}$, and β-arrestin (for review, see (Hedegaard and Holst 2020)). We have recently

JPET Fast Forward. Published on January 11, 2023 as DOI: 10.1124/jpet.122.001393
This article has not been copyedited and formatted. The final version may differ from this version.

investigated a GHSR1a antagonist/inverse agonist, PF-5190457, as a potential therapeutic for AUD. PF-5190457 is a spiro-azetidino-piperidine compound originally identified and optimized by Pfizer Inc. for GHSR1a inverse agonist/antagonist activity as a potential treatment for type 2 diabetes mellitus (Kung, Coffey et al. 2012). PF-5190457 displayed inverse agonist/antagonist activity at GHSR1a both *in vitro* and *ex vivo* (Kung, Coffey et al. 2012, Bhattacharya, Andrews et al. 2014, Kong, Chuddy et al. 2016). Furthermore, PF-5190457 decreased ghrelin-induced growth hormone secretion by 77% and gastric emptying time by 20% in humans at a dose of 100 mg twice daily (BID), providing indirect evidence of GHSR1a engagement in humans (Denney, Sonnenberg et al. 2017). Moreover, in a series of rat experiments, followed by a placebo-controlled Phase 1b human study with heavy drinking male and female participants, we identified that PF-5190457 (50 mg and 100 mg BID) was safe and well-tolerated when co-administered with alcohol, had no effects on alcohol metabolism, and showed potential efficacy in behavioral tasks that suggested potential to reduce alcohol and food craving and attention to cues (Lee, Tapocik et al. 2020).

An unexpected finding from analysis of pooled sera collected during our Phase 1b human study was the identification of a major metabolite of PF-5190457 previously unidentified by liquid chromatography-mass spectrometry (LC-MS) of liver microsomal incubations of PF-5190457. Incubating PF-5190457 in liver cytosol reproduced the metabolite observed in our pooled patient sera analysis, suggesting that this metabolite was produced by metabolism of PF-5190457 via liver cytosolic enzymes (Adusumalli, Jamwal et al. 2019, Adusumalli, Jamwal et al. 2019). Nuclear magnetic resonance (NMR) spectroscopy analysis of this compound revealed that hydroxy addition occurred on the piperidine group of PF-5190457 to form the metabolite, which was named PF-6870961 (**Figure 1**) (Adusumalli, Jamwal et al. 2019a, Adusumalli, Jamwal et al. 2019b). Moreover, liver cytosolic incubation of PF-5190457 with xanthine and aldehyde oxidase inhibitors attenuated production of PF-6870961, suggesting that this metabolite is produced by liver cytosolic xanthine and aldehyde oxidases (Adusumalli, Jamwal et al. 2019b). Because initial screenings of PF-5190457 did not identify PF-6870961 as a major metabolite, the

JPET Fast Forward. Published on January 11, 2023 as DOI: 10.1124/jpet.122.001393
This article has not been copyedited and formatted. The final version may differ from this version.

potential on target/off target effects of PF-6870961 and resulting implications for the overall safety and efficacy of PF-5190457 were unknown. Therefore, we conducted a series of experiments to determine the characteristics of PF-6870961 and further understand the pharmacological profile of PF-5190457. We assessed whether PF-5190457 and/or PF-6870961 alters ghrelin acylation by inhibiting GOAT activity and compared the *in vitro* activity at GHSR1a of PF-5190457, PF-6870961, and the recently discovered endogenous GHSR1a antagonist, liver-expressed antimicrobial peptide-2 (LEAP-2) (Ge, Yang et al. 2018).

2. Methods

2.1 PF-5190457 and PF-6870961 Compounds

In our placebo-controlled Phase 1b human study (Lee, Tapocik et al. 2020), participants were administered PF-5190457 (MW: 512 Da) provided in-kind by Pfizer Inc. (New York, NY USA). For GHSR1a binding affinity studies, PF-5190457 was obtained from a Pfizer provided stock and PF-6870961(MW: 528 Da) was synthesized at the National Institute on Drug Abuse (NIDA) Intramural Research Program using a modified synthetic route to the previously published synthetic route for PF-5190457 (Bhattacharya, Andrews et al. 2014). The metabolite was produced on a gram sale with an overall 55% yield starting from (1*R*)-5-bromoindanam; for a detailed description of the synthesis of PF-6870961, please see (Sulima, Akhlaghi et al. 2021). For GOAT and GHSR1a inhibition experiments, PF-5190457 was purchased from Sigma Aldrich (≥95% purity, PZ0270, St. Louis, MO USA) and PF-6870961 was synthesized at NIDA Intramural Research Program (Sulima, Akhlaghi et al. 2021). Rodent experiments utilized a second batch of PF-6870961 synthesized as a hydrochloride salt for improved solubility, as described in (Sulima, Akhlaghi et al. 2021).

2.2 High throughput screen of PF-6870961

To evaluate off-target effects of the hydroxy metabolite, PF-6870961 was dissolved in 0.1% dimethyl sulfoxide (DMSO) and evaluated across 71 binding and enzyme targets at concentrations of 100

JPET Fast Forward. Published on January 11, 2023 as DOI: 10.1124/jpet.122.001393
This article has not been copyedited and formatted. The final version may differ from this version.

nM and 10000 nM (Eurofins Cerep, Le Bois-l'Évêque, France). Each experiment was performed in duplicate. Compound binding was calculated as % binding inhibition of a radioactive labeled ligand specific for each target. Compound enzyme inhibition was calculated as % inhibition of control enzymatic activity. More than 50% binding or enzyme inhibition was considered a significant effect of PF-6870961 at the target.

A separate screen was conducted for serotonin, dopamine, and opioid receptors, as well as biogenic amine transporters for a total of 13 additional targets (VA Medical Center R&D, Portland, OR, USA). Interaction of PF-6870961 dissolved in 0.1% DMSO with these targets was evaluated at concentrations of 100 nM and 10000 nM for inhibition of a radioligand specific for each target. For this screen, each target was evaluated in triplicate and experiments were repeated at least twice. Non-specific binding was subtracted from all data and specific binding in the presence of drug was normalized to specific binding in the absence of drug.

2.3 Ghrelin O-acyltransferase (GOAT) Activity Assay with PF-5190457 and PF-6870961

Methyl arachidonyl fluorophosphonate (MAFP, Cayman Chemical, Ann Arbor, MI) was diluted in DMSO from a stock in methyl acetate. Octanoyl coenzyme A (octanoyl CoA, CoALA, Austin, TX USA) was diluted to 5 mM in 10 mM Tris-HCl pH 7.0 and stored in low adhesion tubes at -80°C until use. The ghrelin-mimetic $GSSFLC_{NH2}$ peptide substrate was commercially synthesized by Sigma-Genosys (The Woodlands, TX USA) in Pepscreen format. The $GSSFLC_{NH2}$ peptide was solubilized in 1:1 acetonitrile/water solution and stored at -80°C. Peptide concentration was determined spectrophotometrically at 412 nm by reaction of the cysteine thiol with 5,5'dithiobis(2-nitrobenzoic acid) using an ϵ_{412} of 14,150 M^{-1} cm^{-1}(Riddles 1979). Peptide substrates were fluorescently labeled with acrylodan and purified via reverse phase high-performance liquid chromatography (HPLC), as previously reported (Darling, Zhao et al. 2015, Sieburg, Cleverdon et al. 2019). Human GOAT (hGOAT) was expressed and enriched in insect (Sf9) membrane protein fractions using a previously published procedure (Darling, Zhao et al. 2015, McGovern-Gooch, Mahajani et al. 2017, Sieburg, Cleverdon et al. 2019).

JPET Fast Forward. Published on January 11, 2023 as DOI: 10.1124/jpet.122.001393
This article has not been copyedited and formatted. The final version may differ from this version.

Membrane proteins fractions from Sf9 cells expressing hGOAT were thawed on ice, then homogenized by passage through an 18-gauge needle ten times. Assays were performed with 10 µg of membrane protein as determined by Bradford assay. For each set of ten samples, a 440 µL master mix was prepared containing 2.5 mM N-2-hydroxyethylpiperazine-N-2-ethane sulfonic acid (HEPES), 10 µM methyl-arachidonyl fluorophosphate (MAFP), and 110 µg membrane protein. 40 µL of the master mix was aliquoted into each low-adhesion microcentrifuge tube. Compounds PF-6870961 and the previously reported GOAT inhibitor NSM-48 were diluted in DMSO to concentrations of 0.5 mM, 5.0 mM, and 50 mM prior to addition to the reaction mixture (McGovern-Gooch, Mahajani et al. 2017). Due to solubility limitations, compound PF-5190457 was solubilized in DMSO to concentrations of 0.1 mM, 1.0 mM, 1.95 mM prior to addition to the reaction mixture. 1 µL of inhibitor stock and 4 µL DMSO (5 µL of PF-5190457 stocks) were added to each reaction and allowed to preincubate for 30 min at room temperature. Reactions were initiated by the addition of octanoyl CoA (300 µM final concentration) and GSSFLC$_{AcDan}$ peptide (1.5 µM final concentration) to yield a final reaction volume of 50 µL. Reactions were incubated for 30 min at room temperature while sealed and then stopped by addition of 50 µL of 20% acetic acid in isopropanol. Membrane proteins were then removed via precipitation with 16.7 µL of 20% trichloroacetic acid followed by centrifugation (1000 x *g*, 1 min). The supernatant was analyzed via reverse-phase HPLC, as previously described (Sieburg, Cleverdon et al. 2019). GOAT acylation activity was determined by substrate and product peak integration in the presence of either sample or vehicle (DMSO). Percent activity was calculated using the Equations 1 and 2 below:

$$(1)\ \%\ \text{activity} = \frac{\%\ \text{peptide octanoylation in presence of inhibitor}}{\%\ \text{peptide octanoylation in absence of inhibitor}}$$

$$(2)\ \%\ \text{peptide octanoylation} = \frac{\text{fluorescence of octanoylated peptide}}{\text{total peptide fluorescence}}$$

2.4 GHSR1a Membrane Filter Binding Assay (Human, Rat, and Dog)

Ghrelin binding assays were performed in 96-well plates in a final volume of 100 µl containing 250 ng (human or rat) or 2 mg (dog) GHSR1a (from HEK293 tetracycline-inducible cell lines expressing

JPET Fast Forward. Published on January 11, 2023 as DOI: 10.1124/jpet.122.001393
This article has not been copyedited and formatted. The final version may differ from this version.

the growth secretagogue receptor 1a; prepared as membranes) and 50 pM [^{125}I] ghrelin (Perkin Elmer Life Sciences, Waltham, MA, USA NEX-388), plus varying concentrations of test compound or vehicle. 0% effect (ZPE) was defined by blank controls included on each plate and 100% effect (HPE) was defined by wells where 1 mM unlabeled ghrelin was added to maximally displace the radioligand. All reagents were diluted in assay buffer (50 mM HEPES, 10 mM $MgCl_2$, 0.2% bovine serum albumin (BSA), ethylenediaminetetraacetic acid (EDTA)-free protease inhibitors mix, pH 7.4) and reactions were incubated for 90 min at room temperature to allow binding to reach equilibrium. The reactions were transferred to a 0.3% polyethyleneimine (PEI)-treated, 96-well glass fiber filtration plate (Perkin Elmer, 6005174) and washed three times with ice-cold 50 mM Tris, pH 7.5 by vacuum filtration. Plates were allowed to dry overnight at room temperature, and the amount of receptor-ligand complex was determined by liquid scintillation counting using a 1450 Microbeta Trilux (Wallac, Victoria, Australia). Data analysis was performed using a proprietary software package. Briefly, the percent effect for each compound dose (Sample) was calculated from raw data as follows: %Effect = 100-100 x ((Sample-HPE) / (ZPE – HPE)) where HPE and ZPE values are averages of 4 wells each. The compound %effect values were then plotted *vs.* log compound concentration and the K_i was determined as follows: $K_i = IC_{50} / (1 + ([\text{radioligand}] / K_d))$ where the IC_{50} was determined from a standard 4-parameter fit algorithm and the K_d value was specific to the batch of GHSR1a membranes used in the assay.

2.5 GHSR1a Inhibition Assays with PF-5190457, PF-6870961, and LEAP-2

Inositol Phosphate (IP) Turnover Assay: COS-7 cells (ATCC® CRL-1651™) were cultured in Dulbecco's modified Eagle's medium (DMEM) 1885 supplemented with 10% fetal bovine serum (FBS), 1% penicillin/streptomycin, and 2 mM L-glutamine at 37°C in a 10% CO_2 incubator. The cells were seeded at a density of 20,000 cells/well in a 96-well plate and allowed to attach overnight. Cells were then transfected by chloroquine-induced calcium precipitation with pCMV-Tag2B plasmid (Stratagene, La Jolla, CA, USA) containing GHSR-wild type (WT) at a concentration of 0.4 μg DNA/well. The GHSR-WT construct was generated by polymerase chain reaction (PCR) overlap extension with Pfu polymerase

JPET Fast Forward. Published on January 11, 2023 as DOI: 10.1124/jpet.122.001393
This article has not been copyedited and formatted. The final version may differ from this version.

(Promega, Madison, WI, USA), as previously described (Mokrosinski, Frimurer et al. 2012) and verified by DNA sequencing (Eurofins MWG Operon, Huntsville, AL, USA). After five hours, the transfection medium was changed to the cultivation medium (5 µL/mL of Myo-[2-3H(N)]-inositol (Perkin Elmer, Waltham, MA USA)), and the cells were incubated for two days at 37°C in a 10% CO_2 incubator.

Prior to IP accumulation studies, the cells were washed once with 37°C 1x Hank's Balanced Salt Solution (HBSS) buffer. After washing, the cells were incubated at 37°C with 100 µl 37°C 1x HBSS buffer containing 10 mM LiCl and the appropriate ligand (ghrelin: Polypeptide Inc., Hillerød, Denmark; Leap 2: Peptide Institute Inc., Japan; Leap 2 fragments: Schafer-N, Copenhagen, PF-5190457, or PF-6870961) at different concentrations for 90 min. After incubation, the plates were placed on ice, and the cells were lysed with ice cold 10 mM formic acid for at least 30 min. After lysing, the cells were transferred to a white bottomed 96-well plate containing scintillation proximity assay yttrium silicate (SPA-YSI) beads (Perkin Elmer, Waltham, MA USA). Plates were shaken at max speed on a plate shaker for a minimum of 10 min at room temperature, after which the plates were spun at 1500 rpm for 5 min and incubated at room temperature for 4 h prior to measurement. The measurements were performed on a Microbeta plate reader (Perkin Elmer) with a 3 min measuring time. The experiment was completed independently in triplicate.

β-arrestin recruitment assay: The bioluminescence resonance energy transfer (BRET) experiments were carried out as previously described (Spiess, Bagger et al. 2019). Briefly, 24 h after seeding cells in a 6-well plate, 60–80% confluent HEK293 cells were transfected with the following plasmids: GHS-R1a, empty pcDNA3.1(+) vector (negative control), or human glucagon-like peptide-1 receptor (GLP-1R, positive control) in combination with the BRET donors (*Renilla* luciferase−fused arrestins, RLuc8–arrestin-2–Sp1 or RLuc8–arrestin-3–Sp1), the BRET acceptor mem-linker-citrine-SH3, and GPCR kinases 2 (GRK2) to facilitate β-arrestin-1 and β-arrestin-2 recruitment. After 24 h, the cells were washed with phosphate buffered saline (PBS) and resuspended in PBS with 5 mmol/L glucose. 85 µL of cell suspension was added to each well on a 96-well isoplate followed by the addition of (PBS) with 5 µmol/L

coelenterazine h (final concentration). After 10 min at room temperature, increasing concentrations of glucagon-like peptide 1 (GLP-1) were added to the positive control cells. Luminescence was measured with an EnVision plate reader (PerkinElmer, Waltham, MA USA) (RLuc8 at 485 ± 40 nm and yellow fluorescent protein (YFP) at 530 ± 25 nm). The experiment was completed independently in triplicate.

2.6 Food and Locomotor Assays with PF-5190457 and PF-6870961 in Rats

Animals: Adult male (*n* = 15) and female (*n* = 15) Wistar rats were purchased from Charles River (Raleigh, NC, USA) and were 8 weeks old at the beginning of the experiments. The GHSR knock-out (KO) Wistar rats were bred at the NIDA Intramural Research Program (NIDA-IRP) using heterozygous animals. Rats were single-housed and held in temperature- and humidity-controlled rooms on a reverse 12 h/12 h light/dark cycle (lights off at 7:00 AM) and had *ad libitum* access to food and water, except during food intake experiments. All procedures were performed accordingly to the National Institutes of Health Guide for the Care and Use of Laboratory Animals and were approved by the Institutional Animal Care and Use Committee of the NIDA Intramural Research Program.

Food intake: Rats were split into two drug treatment groups, PF-5190457 and PF-6870961. Treatment groups were matched by body weight (kg) and sex (5 males and 5 females *per* group). PF-5190457 was prepared with a few drops of Tween 80 and diluted with saline to yield doses of 5 mg/kg, 10 mg/kg, and 15 mg/kg. PF-6870961 was prepared in the same manner with doses of 2.5 mg/kg, 10 mg/kg, and 40 mg/kg, which were selected based on our observations in humans that PF-6870961 concentrations were ~25% of PF-5190457. Vehicle (0 mg/kg) was prepared with 4% Tween 80 and saline. As a positive control, a third group (*n* = 10; 5 males, 5 females) was treated with 10 mg/kg of the widely used prototype GHSR1a antagonist JMV2959 (Sigma Aldrich, St. Louis, MO, USA). This dose was selected based on previous studies demonstrating reductions in food intake at even lower doses of JMV2959 ((Moulin, Brunel et al. 2013, Gomez and Ryabinin 2014). JMV2959 was diluted with saline and saline served as the vehicle. The injection volume for all drugs was 3 ml/kg bodyweight. Drug administration was intraperitoneal (i.p.) immediately prior to testing. Following a within-subjects, Latin-square design, rats

JPET Fast Forward. Published on January 11, 2023 as DOI: 10.1124/jpet.122.001393
This article has not been copyedited and formatted. The final version may differ from this version.

were given i.p. injections of PF-5190457 or PF-6870961 according to group assignment. In the third cohort, 10 mg/kg JMV2959 and vehicle were administered in a counterbalanced manner. Chow was weighed to the nearest 0.1 g immediately prior to injection and 1 h later. In the satiated condition, rats had *ad libitum* access to standard chow. In the fasted condition, chow was removed for 18 h prior to drug treatment. Drug administrations were separated by at least 24 h. To verify that the any effects of PF-6870961 observed was mediated via GHSR1a, later on an additional experiment was conducted to again assess food intake, in both fed and fasted conditions, following administration of either vehicle or the highest dose of PF-6870961 (40 mg/kg) using a within-subjects design in age-matched (8 wks) male and female GHSR KO Wistar rats. This transgenic CRISPR/Cas9 line of GHSR KO rats was previously developed at the NIDA Intramural Research Program (Zallar, Tunstall et al. 2019b).

Spontaneous locomotion: PF-5190457 was prepared as described above. Due to limited availability of PF-6870961, only the effect of PF-5190457 (30 mg/kg) on spontaneous locomotion was assessed using an open field test. Rats (n = 10; 5 males, 5 females) were first habituated to the apparatus with grey floor and plexiglass walls (40 cm x 40 cm) for 15 min. The next day, rats were administered vehicle or 30 mg/kg PF-5190457 in a randomized order and 30 min later they were put in the center of the open field. Locomotion was recorded for 15 min. One day later, all rats were tested again for locomotion with the opposite vehicle or PF-5190457 treatment of test 1. Open field tests were conducted in a room with red light. Anymaze Video Tracking software (Global Biotech, Mount Laurel, NJ, USA) was used to track total distance traveled (m) and average speed (m/s) of each rat.

Statistical Analysis: Significant outliers were identified using the ROUT method (Q = 1%) and excluded. For food intake experiments, one-way analysis of variance (ANOVA) was used to analyze an effect of dose for PF-5190457- and PF-6870961-treated rats. Paired Student's t-test was used to assess the effect of dose on food intake in JMV2959-treated animals. For spontaneous locomotion, a paired Student's t-test was used to compare PF-5190457 treatment to vehicle. In the case of outlier exclusion, mixed-effects analyses were performed in lieu of ANOVA. If a main effect of treatment was observed, Dunnett *post hoc*

tests were used to determine the significant difference(s). GraphPad Prism Software (San Diego, CA USA) was used for statistical analyses.

2.7 Analysis of PF-6870961 and PF-5190457 Concentration in Humans:

We evaluated the concentration of PF-6870961 in plasma samples of all participants enrolled in our parent Phase 1b human study of PF-5190457, whose main results have been published elsewhere (Lee, Tapocik et al. 2020). Briefly, participants were recruited to the National Institute on Alcohol Abuse and Alcoholism (NIAAA) inpatient unit at the NIH Clinical Center in Bethesda, MD through flyers and advertisements. Potential candidates underwent a phone screen before completing an in-person screen during which a battery of assessments and clinical labs were performed. Male and female participants meeting inclusion criteria consumed >14 and 7 drinks a week, respectively, according to Timeline Followback data. A full description of inclusion and exclusion criteria has been published (Lee, Tapocik et al. 2020) and can also be found in **Supplementary Appendix S1**. The human Phase 1b study was approved by the appropriate Institutional Review Board and conducted under FDA Investigational New Drug 119,365. Each participant provided written informed consent before being enrolled. The study had a within-subject, placebo-controlled, single escalating dose design where patients participated to three separate three-day visits (separated by proper between-visit wash-out periods). During each 3-day visit, PF-5190457 was given five times to reach steady state. Specifically, participants received placebo at the first 3-day visit, 50 mg BID PF-5190457 at the second 3-day visit, and finally 100 mg BID PF-5190457 at the 3rd 3-day visit. Blood samples were collected in the early (8:00 AM) and late (10:45 AM) morning and afternoon of the first two days of each visit. On the third day, multiple blood samples were collected following consumption of a standardized oral alcohol beverage to observe any possible interaction between PF-5190457 and alcohol. Blood was immediately centrifuged at 1700 x g for 15 min at 4°C and extracted plasma was stored at -80 °C until analysis. The concentrations of PF-5190457 and PF-6870961 was determined using a previously published liquid chromatography mass spectrometry (LC-MS) method (Adusumalli, Jamwal et al. 2019a).

JPET Fast Forward. Published on January 11, 2023 as DOI: 10.1124/jpet.122.001393
This article has not been copyedited and formatted. The final version may differ from this version.

Correlation analyses between self-reported food craving scores and plasma concentrations of PF-5190457 and PF-6870961 were conducted using self-report data and blood samples collected on the first and second day of visit 3, where participants received 100 mg BID of PF-5190457. Briefly, for the first two days of a visit, the General Food Craving Questionnaire-State (GFCQ-S) was given before (8:30 AM) and after (10:00 AM) the morning dose of placebo or PF-5190457. On the second day of each visit, a cue reactivity procedure was performed in a bar-like environment in which participants were administered the GFCQ-S following exposure to neutral cues, food-related cues, and alcohol-related cues. Full details and main findings of this procedure have been previously published (Lee, Tapocik et al. 2020). Participants provided information regarding their preferred snack or alcohol beverage at the beginning of the study and these choices served as the food and alcohol cues used during the experiment. To evaluate any preliminary relationship between PF-6870961 or PF-5190457 and food craving, Pearson correlations were calculated between individual metabolite or parent compound concentrations and GFCQ-S scores collected on the first and second day of the last visit (where participants received 100 mg BID PF-5190457) using SPSS (IBM, Armonk, NY). Specifically, correlation scores were calculated between the change in GFCQ-S score (Post-dose or T2 – Pre-dose or T1) and the change in PF-6870961 or PF-5190457 concentration (T2 – T1) on both day 1 and day 2 on visit 3. Additionally, the correlations between Day 2 T2 PF-6870961 or PF-5190457 concentration and GFCQS scores collected during alcohol cue-reactivity following neutral (CR1), food (CR2), and alcohol (CR3) sensory and olfactory cues were calculated. Scatterplots of PF-5190457 and PF-6870961 plasma concentration and GFCQ-S scores were generated in R version 4.1.2 (R Core Team (2022)).

3. Results

3.1 PF-6870961 has no off-target effects in a high-throughput screen

PF-6870961 did not produce greater than 50% inhibition of radioligand binding or control enzymatic activity for all targets tested at both concentrations of 0.1 μM and 10 μM (**Table S1**). Highest inhibition effects were observed for 10000 nM PF-0680961 at D4.4 and choline acetyl transferase,

JPET Fast Forward. Published on January 11, 2023 as DOI: 10.1124/jpet.122.001393
This article has not been copyedited and formatted. The final version may differ from this version.

producing 43.5% and 46.4% inhibition, respectively. Additionally, PF-6870961 did not produce greater than 50% inhibition of radioligand binding at either concentration tested of 0.1 μM and 10 μM for dopamine, opioid, and serotonin receptors and dopamine, serotonin, and norepinephrine transporters (**Table S2**).

3.2 PF-5190457 and PF-06870961 do not inhibit ghrelin O-acyltransferase (GOAT) Activity

To determine whether PF-5190457 and PF-6870961 could interfere with the activity of GOAT, the enzyme that acylates ghrelin, PF-5190457 and PF-6870961 were tested for potential hGOAT inhibitory activity. PF-5190457 was limited in testing due to poor solubility and did not appreciably inhibit hGOAT at the highest tested concentration (~30% inhibition at 195 μM), exhibiting no evidence for concentration-dependent inhibition. PF-6870961 also did not inhibit hGOAT, with less than 20% inhibition at 1000 μM. (**Figure 2**).

3.3 PF-6870961 binds to GHSR1a with lower affinity that PF-5190457

PF-5190457 and PF-680961 binding affinity to GHSR1a was determined in three species (human, rat, dog) in a competitive binding assay using [I^{125}] ghrelin as a radioligand (**Table 1**). For PF-6870961, mean Ki values for human (n = 6), rat (n = 6), and dog (n = 6) GHSR1a was 73.6 nM (95% CI: 52.4 – 103 nM), 239 nM (95% CI: 218 – 262 nM), 217 nM (95% CI: 186 – 253 nM), respectively. For PF-5190457, Ki values calculated from experiments with human (n = 3), rat (n = 3), and dog (n = 3) GHSR1a were 2.96 nM (95% CI: 2.64 – 3.33 nM), 3.94 nM (95% CI: 2.88 – 5.39 nM), and 4.88 nM (95% CI: 4.23 – 5.64 nM), respectively. Data for PF-5190457 was not significantly different from previous data collected by Pfizer on GHSR1a binding affinity (Human: n = 52, Ki = 2.49 nM; Rat: n = 49, Ki = 3.19 nM; Dog: n = 9, Ki = 3.56 nM). Overall, PF-6870961 had approximately 25, 60, and 44-fold lower affinity than PF-5190457 for human, rat, and dog GHSR, respectively.

3.4 PF-6870961 displays inverse agonist and antagonist activity at GHSR1a

JPET Fast Forward. Published on January 11, 2023 as DOI: 10.1124/jpet.122.001393
This article has not been copyedited and formatted. The final version may differ from this version.

PF-6870961 inhibited the constitutive GHSR1a-induced IP accumulation with an IC_{50} values of 300 nM. This was a higher effective concentration than either PF-5190457 or LEAP-2 (the endogenous agonist of GHSR1a), which inhibited constitutive GHSR1a-induced IP mobilization at IC_{50} values of 6.8 nM and 4.7 nM, respectively, suggesting approximately 50-fold lower potency of PF-6870961 at GHSR1a (**Figure 3A-B, Table 2**). However, in the case of GHSR1a-induced β-arrestin mobilization, PF-6870961 had higher inhibitory potency than PF-5190457 and LEAP-2, with an IC_{50} of 1.1 nM for inhibition of GHSR1a constitutive activity (**Figure 3C-D, Table 2**). Constitutive GHSR1a β-arrestin mobilization was inhibited by LEAP-2 with an IC_{50} of 20.5 nM and by PF-5190457 with an IC_{50} of 3.4 nM.

3.5. Both PF-5190457 and PF-6870961 suppress food intake in male and female rats

Initial analyses of the data identified no significant main effect of sex on food intake in each treatment group, therefore the analysis was simplified to either mixed effects analysis or one-way ANOVA depending on the presence of outliers in the sample. Mixed-effects analysis indicated a significant effect of PF-5190457 on food intake (g chow/kg bodyweight) in satiated male and female rats ($F_{4,34} = 3.236$, $p = 0.0236$), and *post hoc* analyses showed that PF-5190457 significantly reduced food intake at 30 mg/kg ($p = 0.0118$) compared with vehicle (**Figure 4A**). Outlier data from two female rats at the 30 mg/kg dose were not included in the analysis. One-way ANOVA showed a significant effect of PF-5190457 on food intake in fasted male and female rats ($F_{4,36} = 2.705$, $p = 0.0455$). PF-5190457 significantly reduced food intake at 30 mg/kg ($p = 0.0222$) compared with vehicle (**Figure 4B)**. Mixed-effects analysis indicated a significant effect of PF-6870961 on food intake in satiated male and female rats ($F_{3,34} = 3.372$, $p = 0.0295$). PF-6870961 significantly reduced food intake at 40 mg/kg *vs.* vehicle ($p = 0.0130$; **Figure 4C).** Outlier data from two female rats at the 40 mg/kg dose were not included in the analysis. Likewise, PF-6870961 significantly reduced food intake in fasted male and female rats ($F_{3,27} = 11.22$, $p < 0.0001$). PF-6870961 significantly reduced food intake at 40 mg/kg *vs.* vehicle ($p = 0.0053$; **Figure 4D**). As a positive control, the GHSR1a antagonist JMV2959 was also tested. A paired t-test showed a significant effect of

JPET Fast Forward. Published on January 11, 2023 as DOI: 10.1124/jpet.122.001393
This article has not been copyedited and formatted. The final version may differ from this version.

10 mg/kg JMV2959 *vs.* vehicle on food intake in the satiated condition ($t_9 = 2.975$, $p = 0.0156$; **Figure 4E**). However, no significant difference was observed for the fasted condition ($t_9 = 0.4673$, $p = 0.6514$; **Figure 4F**). In GHSR KO rats, paired t-test identified no significant difference between vehicle or PF-6870961 (40 mg/kg, i.p.) treated groups on food intake in either satiated ($t_9 = 0.2442$, p = 0.81) or fasted ($t_9 = 1.586$, p = 0.15) conditions (**Figure 5**). A paired t-test showed no significant effect of PF-5190457 on distance traveled ($t_9 = 0.4088$, $p = 0.692$; **Figure S1A**) or average speed ($t_9 = 0.4182$, $p = 0.686$; **Figure S1B)** in the open field.

3.6. Correlation between PF-5190457 and PF-6870961 Concentration and Food Craving in Humans

Demographics for the sample are included in **Table 3.** Average plasma concentrations of PF-5190457 and PF-6870961 for each of the three visits of our Phase 1b study indicated the metabolite circulated at a concentration approximately 25% of the concentration of the parent compound (**Figure 6, Table S3**). Pearson correlations between GFCQ-S scores and plasma concentrations of PF-5190457 and PF-6870961 revealed no correlation between parent or metabolite plasma concentration and self-reported food craving indexed by GFCQ-S (**Figure 7, Table 4**).

4. Discussion

We report the initial pharmacological characterization of PF-6870961, a newly major metabolite of PF-5190457 that we recently discovered. Here, we demonstrated that PF-6870961 exhibits no off-target activity in a full high throughput screen of binding and enzymatic targets. We have demonstrated that PF-6870961 binds to human GHSR1a with approximately 25-fold lower affinity than PF-5190457 and displays inverse agonist at GHSR1a by inhibiting both constitutive GHSR1a activity. Both PF-5190457 and PF-6870961 did not inhibit GOAT enzymatic activity, indicating that both the parent and metabolite compounds do not suppress ghrelin acylation. Lastly, we identified that both parent and metabolite compounds significantly suppress food intake in male and female rats in fed and fasted states.

JPET Fast Forward. Published on January 11, 2023 as DOI: 10.1124/jpet.122.001393
This article has not been copyedited and formatted. The final version may differ from this version.

The GHSR1a is a member of the class B family of 7 transmembrane domain (TMD) GPCRs. Recent structural insight into the binding mechanism of PF-5190457 at GHSR1a indicates that the (6-methylpyrimidin-4-yl)-2,3-dihydro-1 H-inden-1-yl moiety (hydroxylated in PF-6870961) gets pushed into the cleft between TMD2 and TMD3 where it forms hydrophobic and van der Waals interactions with surrounding residues (Qin, Cai et al. 2022). Our observation that PF-6870961 had approximately 25-fold lower affinity for human GHSR1a in a competitive binding assay could therefore be due to the increased polarity of this moiety introduced by the hydroxyl group in a binding pocket, where hydrophobic interactions between the receptor and parent compound are observed. Consistent with our observations of lower affinity, PF-6870961 demonstrated less inverse agonism of GHSR1a-stimulated production of IP. GHSR1a couples to $G\alpha_q$ proteins, which activate phospholipase C (PLC) to stimulate the production of inositol 3,4,5 triphosphate (IP_3) among other downstream effects. To assess inhibitory potency at GHSR1a, we evaluated the ability of both PF-5190457 and PF-6870961 to inhibit constitutive $G\alpha_q$-stimulated production of IP via GHSR1a. PF-6870961 demonstrated 50-fold lower potency at inhibiting constitutive GHSR1a induction of IP, which was not unexpected, due to its lower binding affinity for the receptor. In comparison to the endogenous antagonist of GHSR1a, LEAP-2, PF-5190457 had similar potency against constitutive IP production. It has been shown that alanine substitution for F119 and Q120 (residues that interact with the PF-5190457 moiety that is hydroxylated on the metabolite) significantly reduce inhibition of GHSR1a-stimulated IP_1 accumulation via PF-5190457 (Qin, Cai et al. 2022). This raises the possibility that the introduction of a polar group in this pocket may disrupt hydrophobic interactions with F119 and Q110 necessary for inverse agonism of $G\alpha_q$ stimulated pathways. Still, we found that in the case of GHSR1a-activation of $G\alpha_q$, PF-6870961 is a weak inverse agonist, and that PF-5190457 displays similar potency to LEAP-2.

GHSR1a has been shown to not only couple to $G\alpha_q$, but also $G\alpha_{i/o}$, $G_{12/13}$, and β-arrestin proteins (Hedegaard and Holst 2020). To assess the inhibitory potency of our parent and metabolite compound at a different signaling pathway downstream of GHSR1a, we again compared the effective inhibitory

JPET Fast Forward. Published on January 11, 2023 as DOI: 10.1124/jpet.122.001393
This article has not been copyedited and formatted. The final version may differ from this version.

concentrations of PF-5190457, PF-6870961, and LEAP-2 (the latter being a recently discovered endogenous antagonist of GHSR1a) in the case of constitutive and ghrelin-induced GHSR1a recruitment of β-arrestin (Ge, Yang et al. 2018). We found that PF-6870961 had the lowest effective concentration for both constitutive GHSR1a recruitment of β-arrestin, displaying approximately 20-fold higher potency than LEAP-2 and slightly higher potency (4-7-fold) than PF-5190457. The equivalent potency of the metabolite to the parent compound was unexpected, given the lower affinity and, thus, lower occupancy of the receptor expected at similar concentrations to the parent compound. β-arrestin recruitment to GPCRs occurs through phosphorylation of serine and threonine residues on the C-terminal tail of the active receptor through G-protein coupled receptor kinases (GRKs). The constitutive activity of GPCRs (including constitutive β-arrestin recruitment) often involves conformational flexibility that allows outward movement of TM5 relative to TM3, which permits association with the Gα subunit via interactions with the 7 TM barrel on the intracellular side. This has also been found to be important for constitutive activity of GHSR1a, as mutations disrupting extracellular loop (ECL) 2 flexibility (normally allowing TMD5 movement relative to TMD3) abolished constitutive β-arrestin signaling as well as signaling via other GHSR1a-coupled pathways (Mokrosinski, Frimurer et al. 2012). Our findings therefore add potential structure-activity relationship insight, given that the only structural difference between parent and metabolite compounds is the addition of a hydroxyl group on the piperidine ring, yet the effective inhibitory concentration for the metabolite is much lower than the concentration required for 50% occupancy of the receptor. This observation suggests that the metabolite may have a higher receptor reserve than the parent compound in the case of inverse agonism of GHSR1a-coupled β-arrestin signaling. Although further research is needed, this may be a noteworthy finding for the future design of GHSR1a inverse agonists with reduced tachyphylaxis due to β-arrestin-induced GHSR1a internalization or for biased inverse agonism of β-arrestin coupled signaling pathways. Recently published observations of the binding mechanism of PF-5190457 suggest that the parent moiety hydroxylated on the metabolite interacts with amino acid residues on TMD3 and ECL2 via hydrophobic interactions (Qin, Cai et al. 2022), making it possible that the metabolite forms hydrogen bonds in this region that confer biased

JPET Fast Forward. Published on January 11, 2023 as DOI: 10.1124/jpet.122.001393
This article has not been copyedited and formatted. The final version may differ from this version.

inverse agonism of β-arrestin recruitment, such as through disrupted flexibility of ECL2. Collectively, we have found that PF-5190457 and its metabolite are more potent inhibitors of GHRS1a-induced β-arrestin recruitment, in comparison to LEAP-2. Future studies should compare inhibitory potency of these compounds at GHSR1a-coupled $G_{i/o}$ or $G_{12/13}$ pathways.

To determine whether PF-6870961 demonstrated an *in vivo* effect, we evaluated the acute effect of both parent and metabolite compounds on food intake in male and female rats. Ghrelin can influence food intake by binding to GHSR1a expressed on hypothalamic neurons that stimulate the production of orexin or by binding to GHSR1a expressed on vagal afferent neurons in the stomach (Al Massadi, Nogueiras et al. 2019). We found that both parent and metabolite compounds dose-dependently inhibited food intake in fed (rats that were not food restricted) and fasting (food withheld overnight) conditions. As expected, baseline food intake was higher in the fasted condition. Notably, the widely used prototype GHSR1a antagonist, JMV2959, did not significantly inhibit food intake in the fasted condition but did in the satiated condition. This could be due to JMV2959 only acting as an antagonist at the GHSR1a as opposed to the inverse agonist activity observed with PF-5190457 and PF-6870961. Moreover, increased competition for GHSR1a could be expected under fasting conditions, when endogenous ghrelin is secreted into the peripheral circulation, and may be why no effect of JMV2959 on food intake was observed under fasted conditions. We did not have an a priori hypothesis that the activity of PF-5190457 and PF-6870961 would differ by sex, and therefore did not power our experimental groups accordingly. Analyzing the data via a two-way ANOVA evaluating a main effect of *sex*, *dose*, and *sex X dose* interaction effect identified no significant main effect of sex, thus our analysis was simplified to evaluate only a main effect of treatment. However, because our experiment was likely underpowered to detect an effect of sex on PF-5190457 or PF-6870961 activity, future experiments with larger sample sizes should be performed to more conclusively determine whether the parent and/or metabolite compound have sexually dimorphic efficacy.

JPET Fast Forward. Published on January 11, 2023 as DOI: 10.1124/jpet.122.001393
This article has not been copyedited and formatted. The final version may differ from this version.

Our results suggest that when PF-5190457 is administered to humans, its effects on the receptor would possibly reflect the combined effects of PF-5190457 and its metabolite PF-6870961. This is consistent with our results in rats that preliminarily demonstrated an *in vivo* effect of PF-6870961. The time-concentration profile of PF-5190457 and PF-6870961 in the plasma in humans indicate that the metabolite circulates at approximately 25% of the concentration of the parent compound, at least in humans. The majority of our sample were male participants and all of them met criteria for heavy drinking via 90-day timeline follow back data. Therefore, the metabolism of PF-5190457 should also be evaluated in a sample with larger representation of females as well as lower alcohol consumption to determine whether production of the PF-6870961 metabolite occurs to a different extent in either males or individuals with heavy alcohol drinking. In our Phase 1b human study of PF-5190457, we identified an overall effect of PF-5190457 dose on GFCQ-S self-reported food craving following food cue exposure (Adusumalli, Jamwal et al. 2019a, Adusumalli, Jamwal et al. 2019b, Farokhnia, Portelli et al. 2020, Lee, Farokhnia et al. 2020, Lee, Tapocik et al. 2020, Sulima, Akhlaghi et al. 2021). Specifically, PF-5190457 was significantly associated with lower self-reported GFCQ-S craving. We therefore set out in this manuscript to determine whether there was a relationship between plasma concentrations of PF-5190457 or PF-6870961 and GFCQ-S scores since individual differences in metabolism can lead to varying concentrations of these compounds. Our preliminary analysis of the relationship between PF-5190457 or metabolite concentrations and self-reported food craving in humans revealed no correlation between these variables, but future experiments designed to compare the relationship between metabolite concentrations and food craving would allow for more powerful statistical modeling and adjustment for factors such as age, sex, etc. that may currently be washing out any existing relationship between PF-5190457 and PF-6870961 concentration and food craving. Future studies should directly compare the inhibitory potency of PF-5190457 and PF-6870961 on food intake and assess the potency of both PF-5190457 and its metabolite administered together at expected relative concentrations. Moreover, here we only assessed the *in vivo* effects of PF-5190457 and PF-6870961 following acute administration, so future studies should compare the *in vivo* effects of both parent and metabolite compounds following chronic administration.

JPET Fast Forward. Published on January 11, 2023 as DOI: 10.1124/jpet.122.001393
This article has not been copyedited and formatted. The final version may differ from this version.

Following up on the previous work conducted by our laboratories (Adusumalli, Jamwal et al. 2019a, Adusumalli, Jamwal et al. 2019b, Farokhnia, Portelli et al. 2020, Lee, Farokhnia et al. 2020, Lee, Tapocik et al. 2020, Sulima, Akhlaghi et al. 2021) and other groups (Kung, Coffey et al. 2012, Bhattacharya, Andrews et al. 2014, Kong, Chuddy et al. 2016, Qin, Cai et al. 2022), we expand our understanding of the pharmacological activity of PF-5190457 by demonstrating that its major hydroxy metabolite binds to GHSR1a and displays biased inverse agonism of GHSR1a-induced β-arrestin signaling. We demonstrate that both PF-5190457 and PF-6870961 significantly inhibited food intake in rats at similar doses, indicating an *in vivo* effect of the metabolite. We further demonstrated that the effects of this recently discovered metabolite, PF-6870961, on food intake, are unequivocally mediated by GHSR1a, given the lack of similar effects in an experiment in rats lacking the receptor. Our findings presently suggest that future studies using PF-5190457 should consider additional activity due to formation of the active hydroxy metabolite, PF-6870961, and are relevant for future spiro-azetidino-piperidine leads targeting GHSR1a that may undergo metabolic routes similar to PF-5190457.

5. Author Contributions

Participated in research design: Deschaine S., Akhlaghi F., Hougland J., Koob G., Vendruscolo L., Holst B., Leggio L.

Conducted experiments: Pince C., Hedegaard M., Moose J., Stock I., Adusumalli S.

Contributed new reagents or analytic tools: Sulima A., Rice K.

Performed data analysis: Deschaine S., Pince C., Farokhnia M., Hedegaard M., Stock I., Adusumalli

Wrote or contributed to the writing of the manuscript: Deschaine S. Pince C., Farokhnia M., Moose J., Stock I., Hougland J., Holst B., Vendruscolo L., Leggio L.

6. References:

Adusumalli, S., R. Jamwal, L. Leggio and F. Akhlaghi (2019). "Development and validation of an assay for a novel ghrelin receptor inverse agonist PF-5190457 and its major hydroxy metabolite (PF-6870961) by LC-MS/MS in human plasma." J Chromatogr B Analyt Technol Biomed Life Sci **1130-1131**: 121820.
Adusumalli, S., R. Jamwal, L. Leggio and F. Akhlaghi (2019a). "Development and validation of an assay for a novel ghrelin receptor inverse agonist PF-5190457 and its major hydroxy metabolite (PF-6870961) by LC-MS/MS in human plasma." J Chromatogr B Analyt Technol Biomed Life Sci **1130-1131**: 121820.
Adusumalli, S., R. Jamwal, R. S. Obach, T. F. Ryder, L. Leggio and F. Akhlaghi (2019). "Role of Molybdenum-Containing Enzymes in the Biotransformation of the Novel Ghrelin Receptor Inverse

Agonist PF-5190457: A Reverse Translational Bed-to-Bench Approach." Drug Metab Dispos **47**(8): 874-882.
Adusumalli, S., R. Jamwal, R. S. Obach, T. F. Ryder, L. Leggio and F. Akhlaghi (2019b). "Role of Molybdenum-Containing Enzymes in the Biotransformation of the Novel Ghrelin Receptor Inverse Agonist PF-5190457: A Reverse Translational Bed-to-Bench Approach." Drug Metab Dispos **47**(8): 874-882.
Al Massadi, O., R. Nogueiras, C. Dieguez and J. A. Girault (2019). "Ghrelin and food reward." Neuropharmacology **148**: 131-138.
Bhattacharya, S. K., K. Andrews, R. Beveridge, K. O. Cameron, C. Chen, M. Dunn, D. Fernando, H. Gao, D. Hepworth, V. M. Jackson, V. Khot, J. Kong, R. E. Kosa, K. Lapham, P. M. Loria, A. T. Londregan, K. F. McClure, S. T. Orr, J. Patel, C. Rose, J. Saenz, I. A. Stock, G. Storer, M. VanVolkenburg, D. Vrieze, G. Wang, J. Xiao and Y. Zhang (2014). "Discovery of PF-5190457, a Potent, Selective, and Orally Bioavailable Ghrelin Receptor Inverse Agonist Clinical Candidate." ACS Med Chem Lett **5**(5): 474-479.
Darling, J. E., F. Zhao, R. J. Loftus, L. M. Patton, R. A. Gibbs and J. L. Hougland (2015). "Structure-activity analysis of human ghrelin O-acyltransferase reveals chemical determinants of ghrelin selectivity and acyl group recognition." Biochemistry **54**(4): 1100-1110.
Denney, W. S., G. E. Sonnenberg, S. Carvajal-Gonzalez, T. Tuthill and V. M. Jackson (2017). "Pharmacokinetics and pharmacodynamics of PF-05190457: The first oral ghrelin receptor inverse agonist to be profiled in healthy subjects." Br J Clin Pharmacol **83**(2): 326-338.
Deschaine, S. L. and L. Leggio (2022). "From "Hunger Hormone" to "It's Complicated": Ghrelin Beyond Feeding Control." Physiology (Bethesda) **37**(1): 5-15.
Farokhnia, M., M. L. Faulkner, D. Piacentino, M. R. Lee and L. Leggio (2019). "Ghrelin: From a gut hormone to a potential therapeutic target for alcohol use disorder." Physiol Behav **204**: 49-57.
Farokhnia, M., E. N. Grodin, M. R. Lee, E. N. Oot, A. N. Blackburn, B. L. Stangl, M. L. Schwandt, L. A. Farinelli, R. Momenan, V. A. Ramchandani and L. Leggio (2018). "Exogenous ghrelin administration increases alcohol self-administration and modulates brain functional activity in heavy-drinking alcohol-dependent individuals." Mol Psychiatry **23**(10): 2029-2038.
Farokhnia, M., J. Portelli, M. R. Lee, G. R. McDiarmid, V. Munjal, K. M. Abshire, J. T. Battista, B. D. Browning, S. L. Deschaine, F. Akhlaghi and L. Leggio (2020). "Effects of exogenous ghrelin administration and ghrelin receptor blockade, in combination with alcohol, on peripheral inflammatory markers in heavy-drinking individuals: Results from two human laboratory studies." Brain Res **1740**: 146851.
Ge, X., H. Yang, M. A. Bednarek, H. Galon-Tilleman, P. Chen, M. Chen, J. S. Lichtman, Y. Wang, O. Dalmas, Y. Yin, H. Tian, L. Jermutus, J. Grimsby, C. M. Rondinone, A. Konkar and D. D. Kaplan (2018). "LEAP2 Is an Endogenous Antagonist of the Ghrelin Receptor." Cell Metab **27**(2): 461-469 e466.
Gomez, J. L. and A. E. Ryabinin (2014). "The effects of ghrelin antagonists [D-Lys(3)]-GHRP-6 or JMV2959 on ethanol, water, and food intake in C57BL/6J mice." Alcohol Clin Exp Res **38**(9): 2436-2444.
Hedegaard, M. A. and B. Holst (2020). "The Complex Signaling Pathways of the Ghrelin Receptor." Endocrinology **161**(4).
Holst, B., A. Cygankiewicz, T. H. Jensen, M. Ankersen and T. W. Schwartz (2003). "High constitutive signaling of the ghrelin receptor--identification of a potent inverse agonist." Mol Endocrinol **17**(11): 2201-2210.
Jerlhag, E., E. Egecioglu, S. Landgren, N. Salome, M. Heilig, D. Moechars, R. Datta, D. Perrissoud, S. L. Dickson and J. A. Engel (2009). "Requirement of central ghrelin signaling for alcohol reward." Proc Natl Acad Sci U S A **106**(27): 11318-11323.
Kaur, S. and A. E. Ryabinin (2010). "Ghrelin receptor antagonism decreases alcohol consumption and activation of perioculomotor urocortin-containing neurons." Alcohol Clin Exp Res **34**(9): 1525-1534.
Kong, J., J. Chuddy, I. A. Stock, P. M. Loria, S. V. Straub, C. Vage, K. O. Cameron, S. K. Bhattacharya, K. Lapham, K. F. McClure, Y. Zhang and V. M. Jackson (2016). "Pharmacological characterization of the first

in class clinical candidate PF-05190457: a selective ghrelin receptor competitive antagonist with inverse agonism that increases vagal afferent firing and glucose-dependent insulin secretion ex vivo." Br J Pharmacol **173**(9): 1452-1464.
Kung, D. W., S. B. Coffey, R. M. Jones, S. Cabral, W. Jiao, M. Fichtner, P. A. Carpino, C. R. Rose, R. F. Hank, M. G. Lopaze, R. Swartz, H. T. Chen, Z. Hendsch, B. Posner, C. F. Wielis, B. Manning, J. Dubins, I. A. Stock, S. Varma, M. Campbell, D. DeBartola, R. Kosa-Maines, S. J. Steyn and K. F. McClure (2012). "Identification of spirocyclic piperidine-azetidine inverse agonists of the ghrelin receptor." Bioorg Med Chem Lett **22**(13): 4281-4287.
Landgren, S., J. A. Simms, P. Hyytia, J. A. Engel, S. E. Bartlett and E. Jerlhag (2012). "Ghrelin receptor (GHS-R1A) antagonism suppresses both operant alcohol self-administration and high alcohol consumption in rats." Addict Biol **17**(1): 86-94.
Lee, M. R., M. Farokhnia, E. Cobbina, A. Saravanakumar, X. Li, J. T. Battista, L. A. Farinelli, F. Akhlaghi and L. Leggio (2020). "Endocrine effects of the novel ghrelin receptor inverse agonist PF-5190457: Results from a placebo-controlled human laboratory alcohol co-administration study in heavy drinkers." Neuropharmacology **170**: 107788.
Lee, M. R., J. D. Tapocik, M. Ghareeb, M. L. Schwandt, A. A. Dias, A. N. Le, E. Cobbina, L. A. Farinelli, S. Bouhlal, M. Farokhnia, M. Heilig, F. Akhlaghi and L. Leggio (2020). "The novel ghrelin receptor inverse agonist PF-5190457 administered with alcohol: preclinical safety experiments and a phase 1b human laboratory study." Mol Psychiatry **25**(2): 461-475.
Leggio, L., W. H. Zywiak, S. R. Fricchione, S. M. Edwards, S. M. de la Monte, R. M. Swift and G. A. Kenna (2014). "Intravenous ghrelin administration increases alcohol craving in alcohol-dependent heavy drinkers: a preliminary investigation." Biol Psychiatry **76**(9): 734-741.
McGovern-Gooch, K. R., N. S. Mahajani, A. Garagozzo, A. J. Schramm, L. G. Hannah, M. A. Sieburg, J. D. Chisholm and J. L. Hougland (2017). "Synthetic Triterpenoid Inhibition of Human Ghrelin O-Acyltransferase: The Involvement of a Functionally Required Cysteine Provides Mechanistic Insight into Ghrelin Acylation." Biochemistry **56**(7): 919-931.
Mokrosinski, J., T. M. Frimurer, B. Sivertsen, T. W. Schwartz and B. Holst (2012). "Modulation of constitutive activity and signaling bias of the ghrelin receptor by conformational constraint in the second extracellular loop." J Biol Chem **287**(40): 33488-33502.
Morris, L. S., V. Voon and L. Leggio (2018). "Stress, Motivation, and the Gut-Brain Axis: A Focus on the Ghrelin System and Alcohol Use Disorder." Alcohol Clin Exp Res.
Moulin, A., L. Brunel, D. Boeglin, L. Demange, J. Ryan, C. M'Kadmi, S. Denoyelle, J. Martinez and J. A. Fehrentz (2013). "The 1,2,4-triazole as a scaffold for the design of ghrelin receptor ligands: development of JMV 2959, a potent antagonist." Amino Acids **44**(2): 301-314.
Qin, J., Y. Cai, Z. Xu, Q. Ming, S. Y. Ji, C. Wu, H. Zhang, C. Mao, D. D. Shen, K. Hirata, Y. Ma, W. Yan, Y. Zhang and Z. Shao (2022). "Molecular mechanism of agonism and inverse agonism in ghrelin receptor." Nat Commun **13**(1): 300.
Riddles, P. W. B., R. L.; Zerner, B., (1979). "Ellman's reagent: 5,5'-dithiobis(2-nitrobenzoic acid)--a reexamination." Analytical Biochemistry **94**(1): 75-81.
Sieburg, M. A., E. R. Cleverdon and J. L. Hougland (2019). "Biochemical Assays for Ghrelin Acylation and Inhibition of Ghrelin O-Acyltransferase." Methods Mol Biol **2009**: 227-241.
Spiess, K., S. O. Bagger, L. J. Torz, K. H. R. Jensen, A. L. Walser, J. M. Kvam, A. K. Mogelmose, V. Daugvilaite, R. K. Junnila, G. M. Hjorto and M. M. Rosenkilde (2019). "Arrestin-independent constitutive endocytosis of GPR125/ADGRA3." Ann N Y Acad Sci **1456**(1): 186-199.
Suchankova, P., P. Steensland, I. Fredriksson, J. A. Engel and E. Jerlhag (2013). "Ghrelin receptor (GHS-R1A) antagonism suppresses both alcohol consumption and the alcohol deprivation effect in rats following long-term voluntary alcohol consumption." PLoS One **8**(8): e71284.

Sulima, A., F. Akhlaghi, L. Leggio and K. C. Rice (2021). "Synthesis of PF-6870961, a major hydroxy metabolite of the novel ghrelin receptor inverse agonist PF-5190457." Bioorg Med Chem **50**: 116465.
Team, R. C. (2022). R: A Language and Environment for Statistical Computing. R Foundation for Statistical Computing.
Yanagi, S., T. Sato, K. Kangawa and M. Nakazato (2018). "The Homeostatic Force of Ghrelin." Cell Metab **27**(4): 786-804.
You, Z. B., E. Galaj, F. Alen, B. Wang, G. H. Bi, A. R. Moore, T. Buck, M. Crissman, S. Pari, Z. X. Xi, L. Leggio, R. A. Wise and E. L. Gardner (2022). "Involvement of the ghrelin system in the maintenance and reinstatement of cocaine-motivated behaviors: a role of adrenergic action at peripheral beta1 receptors." Neuropsychopharmacology **47**(8): 1449-1460.
Zallar, L. J., S. Beurmann, B. J. Tunstall, C. M. Fraser, G. F. Koob, L. F. Vendruscolo and L. Leggio (2019). "Ghrelin receptor deletion reduces binge-like alcohol drinking in rats." J Neuroendocrinol **31**(7): e12663.
Zallar, L. J., S. Beurmann, B. J. Tunstall, C. M. Fraser, G. F. Koob, L. F. Vendruscolo and L. Leggio (2019a). "Ghrelin receptor deletion reduces binge-like alcohol drinking in rats." J Neuroendocrinol **31**(7): e12663.
Zallar, L. J., M. Farokhnia, B. J. Tunstall, L. F. Vendruscolo and L. Leggio (2017). "The Role of the Ghrelin System in Drug Addiction." Int Rev Neurobiol **136**: 89-119.
Zallar, L. J., B. J. Tunstall, C. T. Richie, Y. J. Zhang, Z. B. You, E. L. Gardner, M. Heilig, J. Pickel, G. F. Koob, L. F. Vendruscolo, B. K. Harvey and L. Leggio (2019b). "Development and initial characterization of a novel ghrelin receptor CRISPR/Cas9 knockout wistar rat model." Int J Obes (Lond) **43**(2): 344-354.

Footnotes:

Funding /Acknowledgements:

We would like to thank Kimberly Whiting (NIDA Intramural Research Program) for her assistance with data collection. We would additionally like to thank Dr. R. Scott Obach (Pfizer, Inc.) for his contributions to initial characterization of PF-6870961, which are cited in this manuscript. We would also like to acknowledge Dr. Amy Newman (NIDA Intramural Research Program) for her support with the high throughput screening of PF-6870961.

This work was funded by 1) the NIDA/NIAAA joint Clinical Psychoneuroendocrinology and Neuropsychopharmacology Section (PI: Lorenzo Leggio); 2) the NIDA Neurobiology of Addiction Section (PI: George F. Koob); and 3) the NIDA/NIAAA joint Drug Design and Synthesis Section (PI: Kenner Rice). Part of this work was also funded by the National Center for Advancing Translational Sciences (NCATS), under an UH2/UH3 grant (TR000963 - PIs: Lorenzo Leggio and Fatemeh Akhlaghi). Part of this work was funded under an NIGMS grant [R01GM134102 - PI: James Hougland]. We also

received support from the NIDA IRP Medication Development Program. Drs Ingrid Stock is a Pfizer employee. Pfizer did not have any role in the study design, execution or interpretation of the results, and this publication does not necessarily represent the official views of Pfizer.

Conflict of Interest Statement

The authors declare that they have no conflicts of interest.

Data Availability Statement: The data that support the findings of this study are available from the corresponding author upon reasonable request. Some data may not be made available because of privacy or ethical restrictions.

List of Abbreviations

- **ANOVA = analysis of variance**
- **AUD = alcohol use disorder**
- **BOLD = blood oxygen level dependent**
- **BRET = bioluminescent resonance energy transfer**
- **BSA = bovine serum albumin**
- **CoA = coenzyme A**
- **CI = confidence interval**
- **DMSO = dimethyl sulfoxide**
- **D4.4 = dopamine receptor 4**
- **DMEM = Dulbecco's modified Eagle's medium**
- **ECL = extracellular loop**
- **fMRI = functional magnetic resonance imaging**
- **GFCQ-S = general food craving questionnaire – state**
- **GPCR = G-protein coupled receptor**
- **GHSR1a = growth hormone secretagogue receptor 1a**

JPET Fast Forward. Published on January 11, 2023 as DOI: 10.1124/jpet.122.001393
This article has not been copyedited and formatted. The final version may differ from this version.

- **GHSR = growth hormone secretagogue receptor**
- **GOAT = ghrelin O-acyltransferase**
- **GRK2 = GPCR kinases 2**
- **GLP-1 = glucagon-like peptide 1**
- **GLP-1R = glucagon-like peptide 1 receptor**
- **hGOAT = human ghrelin O-acyltransferase**
- **HPLC = high performance liquid chromatography**
- **HBSS = Hank's buffered salt solution**
- **HPE = hundred percent effect**
- **IP = inositol phosphate**
- **IP3 = inositol 3,4,5-triphosphate**
- **LC-MS = liquid chromatography mass spectrometry**
- **LEAP-2 = liver-expressed antimicrobial peptide**
- **MAFP = methyl arachidonyl fluorophosphate**
- **PEI = polyethyleneimine**
- **PLC = phospholipase C**
- **PBS = phosphate buffered saline**
- **SH3 = SRC homology 3 domain**
- **SPA-YSI = scintillation proximity assay yttrium silicate**
- **TMD = transmembrane domain**
- **WT = wild-type**
- **YFP = yellow fluorescent protein**
- **ZPE = zero percent effect**

Legends for Figures

JPET Fast Forward. Published on January 11, 2023 as DOI: 10.1124/jpet.122.001393
This article has not been copyedited and formatted. The final version may differ from this version.

Figure 1: Structure of PF-5190457 and PF-6870961. PF-5190457 is converted to PF-6870961 through the addition of a hydroxy group to the piperidine ring. This reaction occurs via cytosolic enzymes, namely xanthine and aldehyde oxidases.

Figure 2: Inhibition of hGOAT by GSHR-1a inverse agonist PF-5190457, metabolite PF-6870961, and known hGOAT inhibitor NSM-48. (A) Effect of PF-5190457 at 10-195 μM and PF-6870961 at 10-1000 μM in comparison to known GOAT inhibitor, NSM-48, at 10–1000 μM. %hGOAT activity = octanoylation of ghrelin mimetic $GSSFLC_{NH2}$ peptide in presence of inhibitor expressed as a percentage of that in the absence of inhibitor and is normalized to vehicle condition. (**B**) Structure of NSM-48 provided for reference. Data represent mean and individual values from independent experiments. n = 2-4. hGOAT = human ghrelin O-acyltransferase

Figure 3: Inhibition of GHSR1a-induced IP mobilization and β-arrestin mobilization by PF-5190457, PF-6870961, and LEAP-2. Concentration response assay to assess inhibitory potency of compounds at GHSR1a expressed on HEK293 cells (**A**) Inhibition of constitutive GHSR1a inositol phosphate (IP) mobilization in the presence of increasing concentrations of PF-5190457, PF-6870961, or LEAP-2. (**B**) Inhibition of GHSR1a IP mobilization as a percentage of the maximal ghrelin-induced response in the presence of increasing concentrations of PF-5190457, PF-6870961, or LEAP-2. (**C**) Inhibition of constitutive GHSR1a β-arrestin recruitment in the presence of increasing concentrations of PF-5190457, PF-6870961, or LEAP-2. (**D**) Inhibition of GHSR1a β-arrestin recruitment as a percentage of the maximal ghrelin-induced response in the presence of increasing concentrations of PF-5190457, PF-6870961, or LEAP-2 Data represent Mean ± SEM. n = 3. β-arrestin = β-arrestin 1 and β-arrestin 2, GHSR1a = growth hormone secretagogue receptor 1a, IP = inositol phosphate, LEAP-2 = liver expressed antimicrobial peptide-2.

Figure 4: Effect of PF-5190457, PF-6870961, and JMV2959 on food intake in satiated and fasted male and female rats. PF-5190457 effect on food intake in satiated (**A**) and fasted (**B**) male and female rats 1 h post-injection relative to baseline. PF-6870961 reduced food intake in satiated (**C**) and fasted (**D**) male and female rats 1 h post-injection. JMV2959 reduced food intake in satiated (**E**) but not fasted (**F**) male and female rats 1 h post-treatment. (**G**) Structure of JMV2959, PF-5190457, and PF-6870961 included for reference. Data represent mean ± S.E.M. * $p < 0.05$, ** $p < 0.01$, difference from vehicle. n = 10, ○ = male rats, ▲ = female rats.

Figure 5: Lack of effect of PF-6870961 on food intake in satiated and fasted male and female GHSR KO rats. PF-6870961 (40mg/kg) vs. vehicle effect on food intake in satiated (A) and fasted (B) male and female rats 1 h post injection. Data represent mean ± S.E.M. p = ns, difference from vehicle. n = 10, ○ = male rats, ▲ = female rats.

Figure 6: Time concentration profile of plasma PF-5190457 and PF-6870961 levels in humans after repeated administrations of PF-5190457. Geometric mean plasma concentration-time PK profile of **(A)** the parent drug PF-5190457 and **(B)** the metabolite PF-6870961, after repeated dosing of PF-5190457 (0 mg BID, 50 mg BID, and 100 mg BID) in our placebo-controlled Phase 1b human laboratory study in male and female individuals with heavy alcohol drinking. Dosing phase: -3000 to 0 minutes; alcohol session phase: 0 to 1440 minutes. N = 14. *Note: The Y-axis of (B) is expanded to show more detail.*

Figure 7: Scatterplots of self-reported food craving vs. PF-5190457 or PF-6870961 plasma concentration in humans. Scatterplots depicting PF-5190457 (ng/mL) (top, green) and PF-6870961 (ng/mL) (bottom, purple) vs. GFCQ-S food craving measures during Visit 3 (where subjects received 100 mg BID PF-5190457). CR = Cue Reactivity. CR T1 = post-neutral cue, CR T2 = post food cue, CR T3 =

JPET Fast Forward. Published on January 11, 2023 as DOI: 10.1124/jpet.122.001393
This article has not been copyedited and formatted. The final version may differ from this version.

post- alcohol cue, GFCQ-S = general food craving questionnaire – state, T2 = post-dose, T1 = pre-dose. N = 12.

Tables:

Table 1: Binding affinity of PF-5190457 and PF-6870961 to GHSR

	Hill Slope	Ki (nM)	95% CI Lower Limit (nM)	95% CI Upper Limit (nM)
PF-5190457				
Human GHSR	1.061	2.96	2.64	3.33
Rat GHSR	0.947	3.94	2.88	5.39
Dog GHSR	1.251	4.88	4.23	5.64
PF-6870961				
Human GHSR	0.789	73.6	52.4	103
Rat GHSR	0.811	239	218	262
Dog GHSR	0.929	217	186	253

GHSR = Growth hormone secretagogue receptor, CI = confidence interval

Table 2: Inhibition of GHSR1a induced IP_3 and β-arrestin mobilization by LEAP-2, PF-5190457, and PF-6870961

	Normalized to Constitutive GHSR1a Activity			*Normalized to 100% Ghrelin-Induced Activity*			
	LEAP-2	**PF-5190457**	**PF-6870961**	**Ghrelin**	**LEAP-2**	**PF-5190457**	**PF-6870961**
IP							
Bottom	7.738	-0.93520	-7.797	53.95	5.869	-0.6585	-4.356
Top	98.81	98.61	100.1	97.09	54.17	61.78	59.26
Hill Slope	-1.966	-1.073	-0.7264	1.192	-1.795	-1.039	-0.7219
EC_{50} (M)	-	-	-	6.58×10^{-10}	-	-	-
IC_{50} (M)	4.77×10^{-9}	6.76×10^{-9}	3.01×10^{-7}	-	5.14×10^{-9}	6.87×10^{-9}	2.752×10^{-7}
Span	91.07	99.54	107.9	43.14	48.30	62.44	63.62
β-Arrestin							
Bottom	-2.582	0.000	0.000	16.12	17.97	17.91	26.20
Top	99.65	100.0	100.0	102.5	-0.5703	1.769	3.128
Hill Slope	-1.154	-1.000	-1.000	1.00	-1.00	-1.00	-1.00
EC_{50}(M)	-	-	-	1.56×10^{-8}	-	-	-
IC_{50} (M)	2.05×10^{-8}	3.39×10^{-9}	1.10×10^{-9}	-	1.98×10^{-8}	7.23×10^{-9}	1.26×10^{-9}
Span	102.2	100.0	100.0	86.40	-18.54	-16.14	-23.07

LEAP-2 = liver expressed antimicrobial peptide-2; GHSR1a = growth hormone secretagogue receptor 1a, IP = inositol phosphate

JPET Fast Forward. Published on January 11, 2023 as DOI: 10.1124/jpet.122.001393
This article has not been copyedited and formatted. The final version may differ from this version.

Table 3: Baseline characteristics of participants in analysis of plasma concentrations of PF-5190457 and PF-6870961

Sample size, N	**12**
Male, N (%)	**11 (91.7)**
Race, N (%)	
African American	**11 (91.7)**
White	**1 (8.3)**
Smoking Status, N (%)	
Smoking	**9 (75.0)**
Non-smoking	**3 (25.0)**
BMI, kg/m^2 (Mean ± SEM)	**26.9 ± 1.3**
Education, yrs (Mean ± SEM)	**12.1 (1.0)**
Age, yrs (Mean ± SEM)	**40 ± 3.8**
90 Day DDD* (Mean ± SEM)	**11.3 ± 3.8**

*from 90-day timeline followback (TLFB), DDD = drinks per drinking day, BMI = body mass index.

Table 4: Correlations between self-reported food craving and PF-5190456 and PF-6870961 plasma concentration

Comparison	Blood Draw Timepoint		GFCQ-S Timepoint	Pearson's Correlation	P value	Sample size (N)
PF-5190457(ng/mL) vs. GFCQS score						
	Day 1: T2 – T1	*vs.*	Day 1: T2 – T1	-0.116	0.719	12
	Day 2: T2 – T1	*vs.*	Day 2: T2 – T1	0.153	0.635	12
	Day 2 T2	*vs.*	Day 2: CR2-CR1	0.431	0.162	12
	Day 2 T2	*vs.*	Day 2: CR3-CR1	0.022	0.945	12
PF-6870961(ng/mL) vs. GFCQS score	Day 1: T2 – T1	*vs.*	Day 1: T2 – T1	0.112	0.728	12
	Day 2: T2 – T1	*vs.*	Day 2: T2 – T1	-0.095	0.768	12
	Day 2 T2	*vs.*	Day 2: CR2-CR1	-0.015	0.963	12
	Day 2 T2	*vs.*	Day 2: CR3-CR1	0.000	1.000	12

Pearson correlation values calculated between individual metabolite concentrations and GFCQ-S scores at different time points during Visit 3 (subjects received 100 mg BID PF-5190457). CR = Cue Reactivity. CR T1 = post-neutral cue, CR T2 = post food cue, CR T3 = post- alcohol cue, GFCQ-S = general food craving questionnaire – state, T2 = post-dose, T1 = pre-dose. N = 12.

Figures:

Figure 1

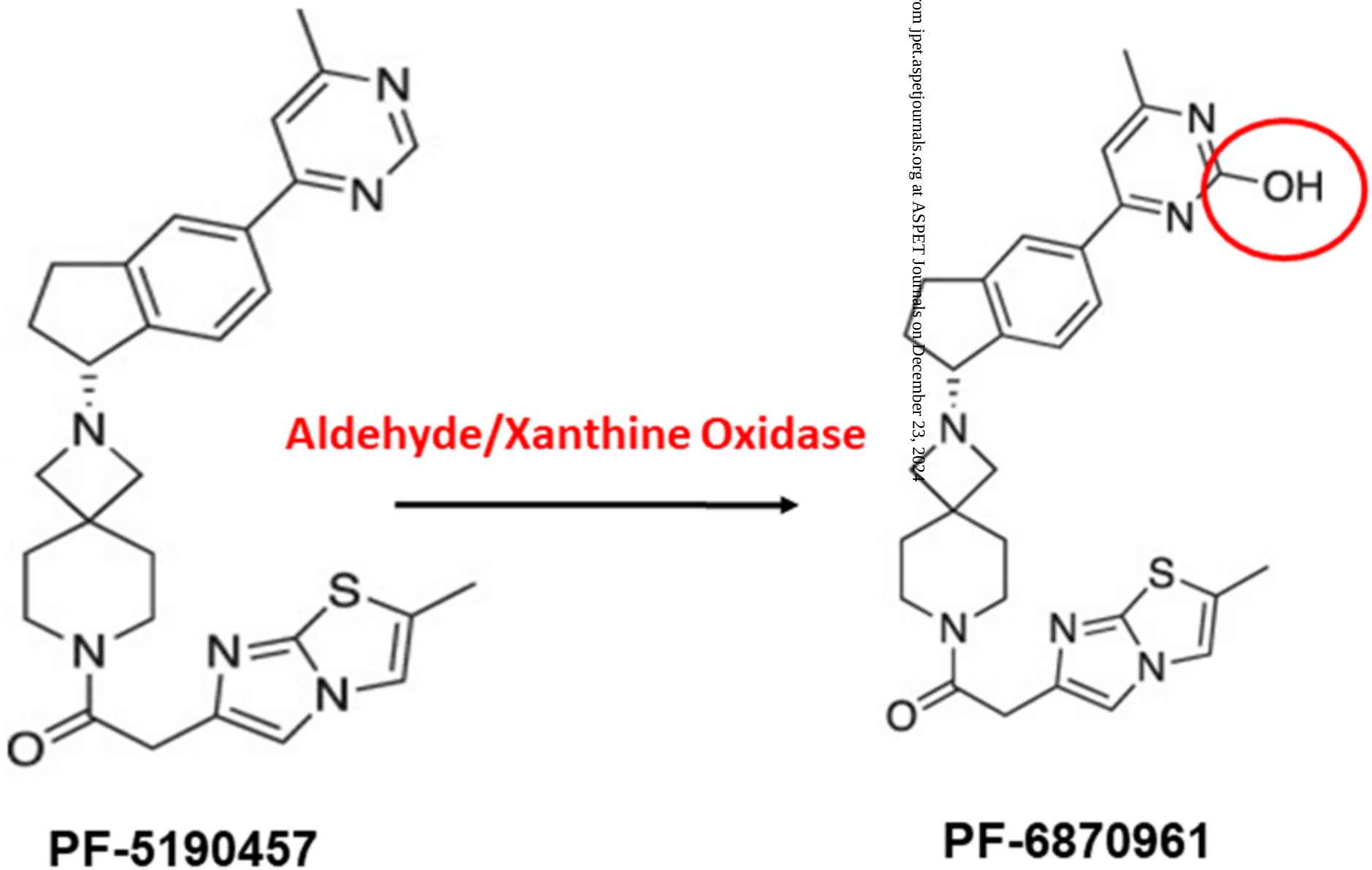

Figure 2

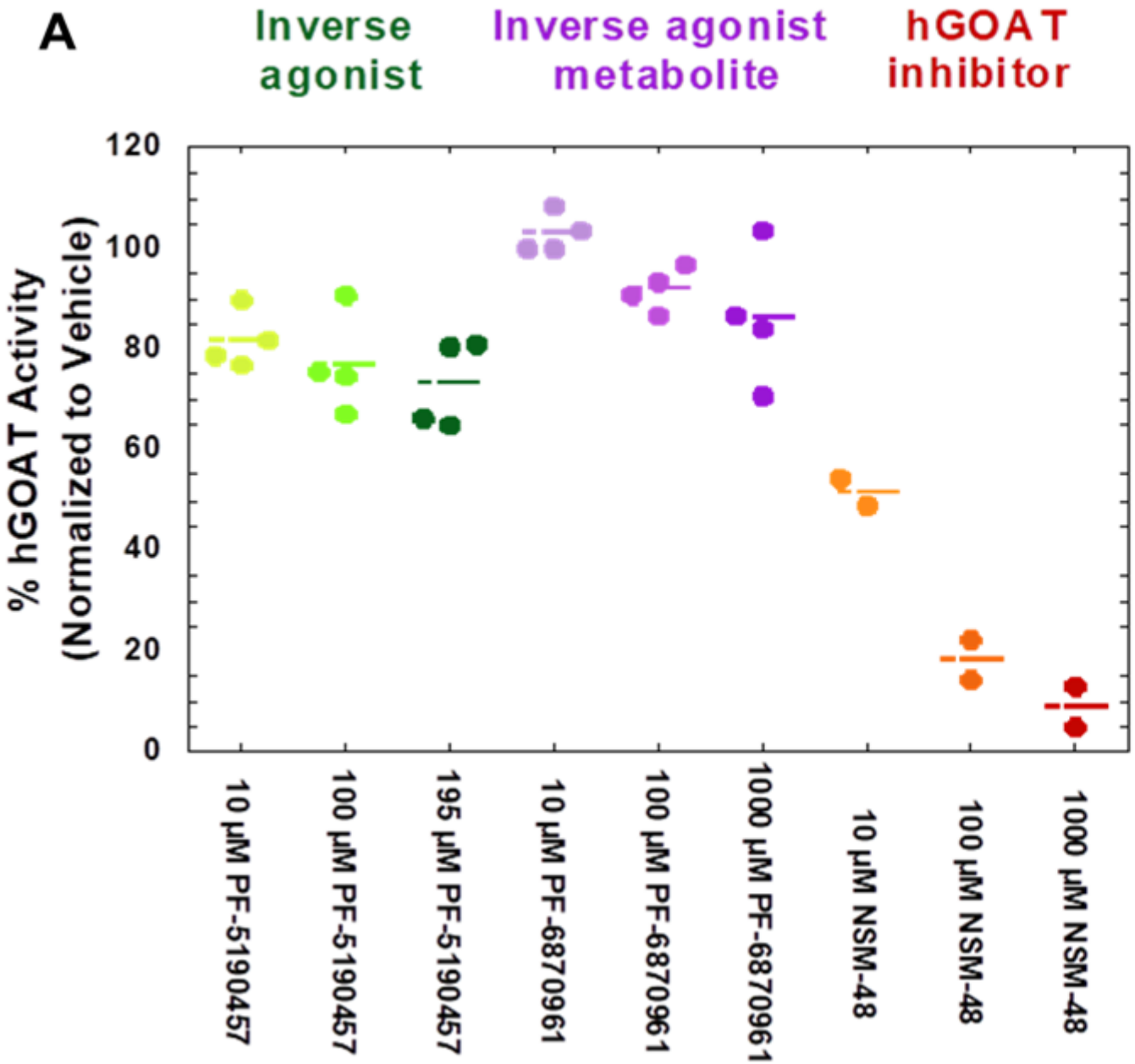

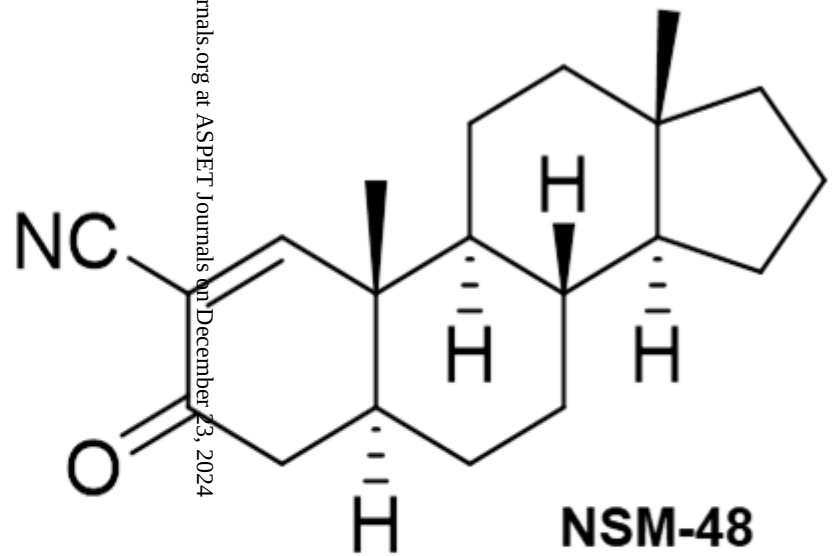

Figure 3

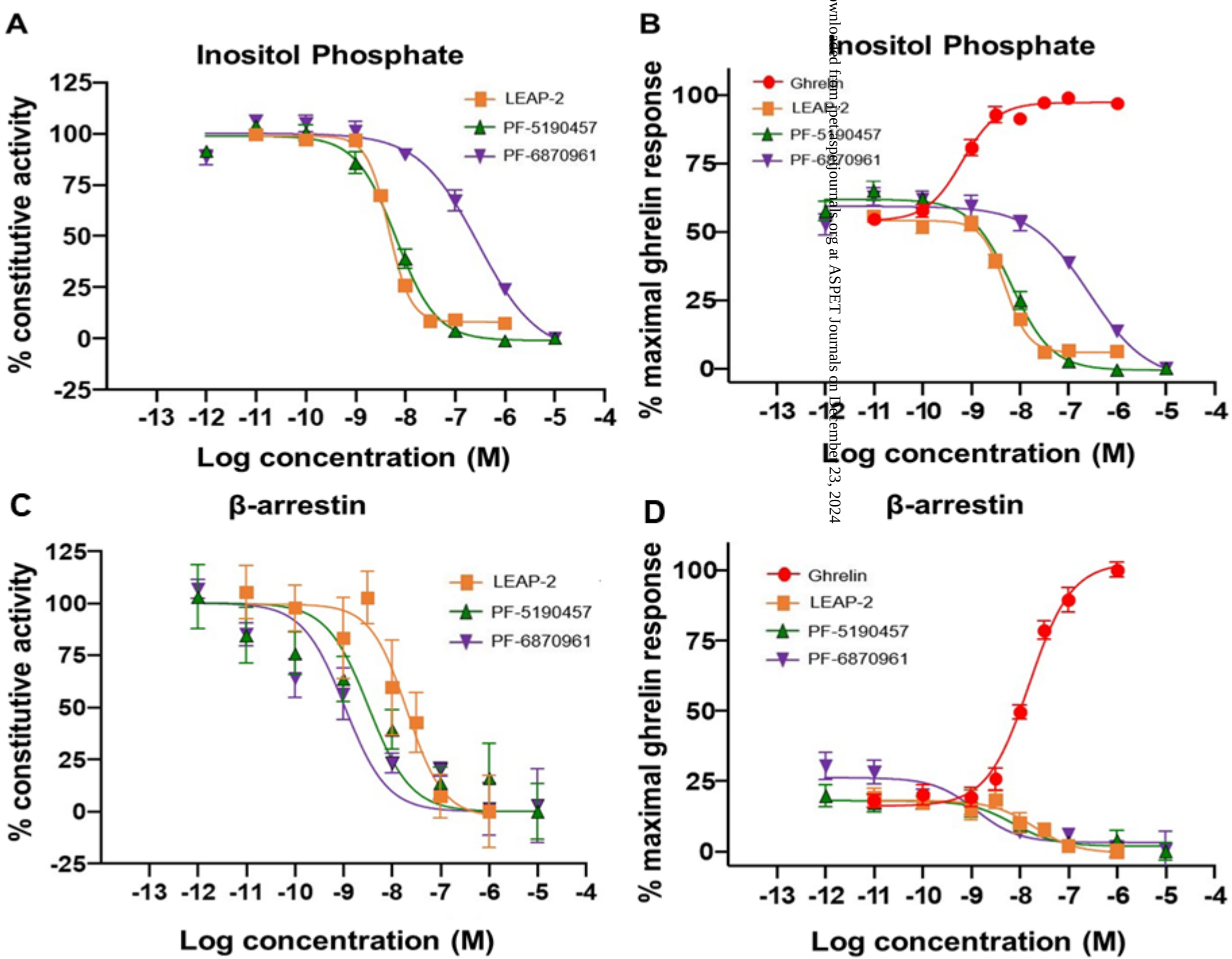

Figure 4

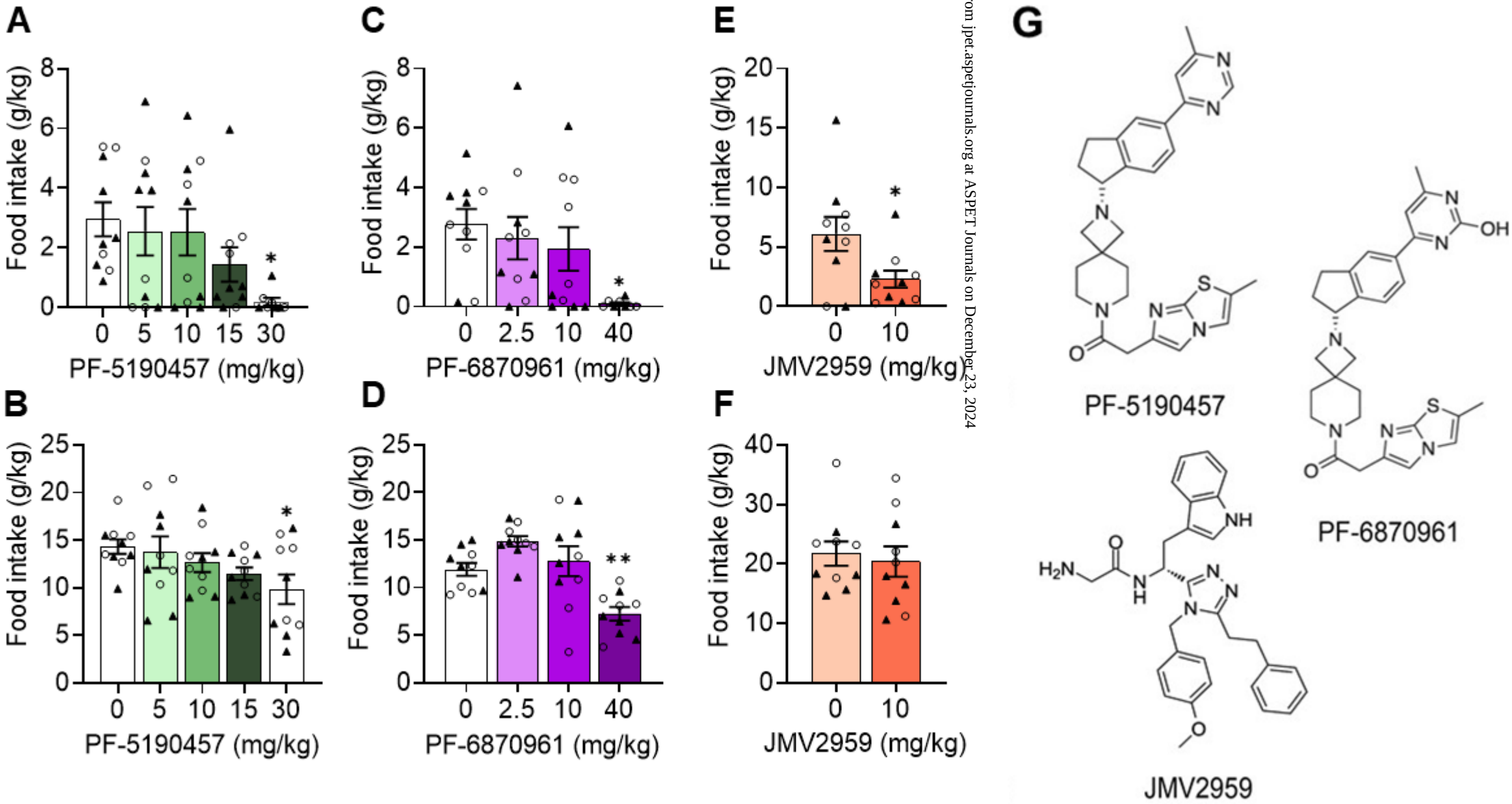

Figure 5

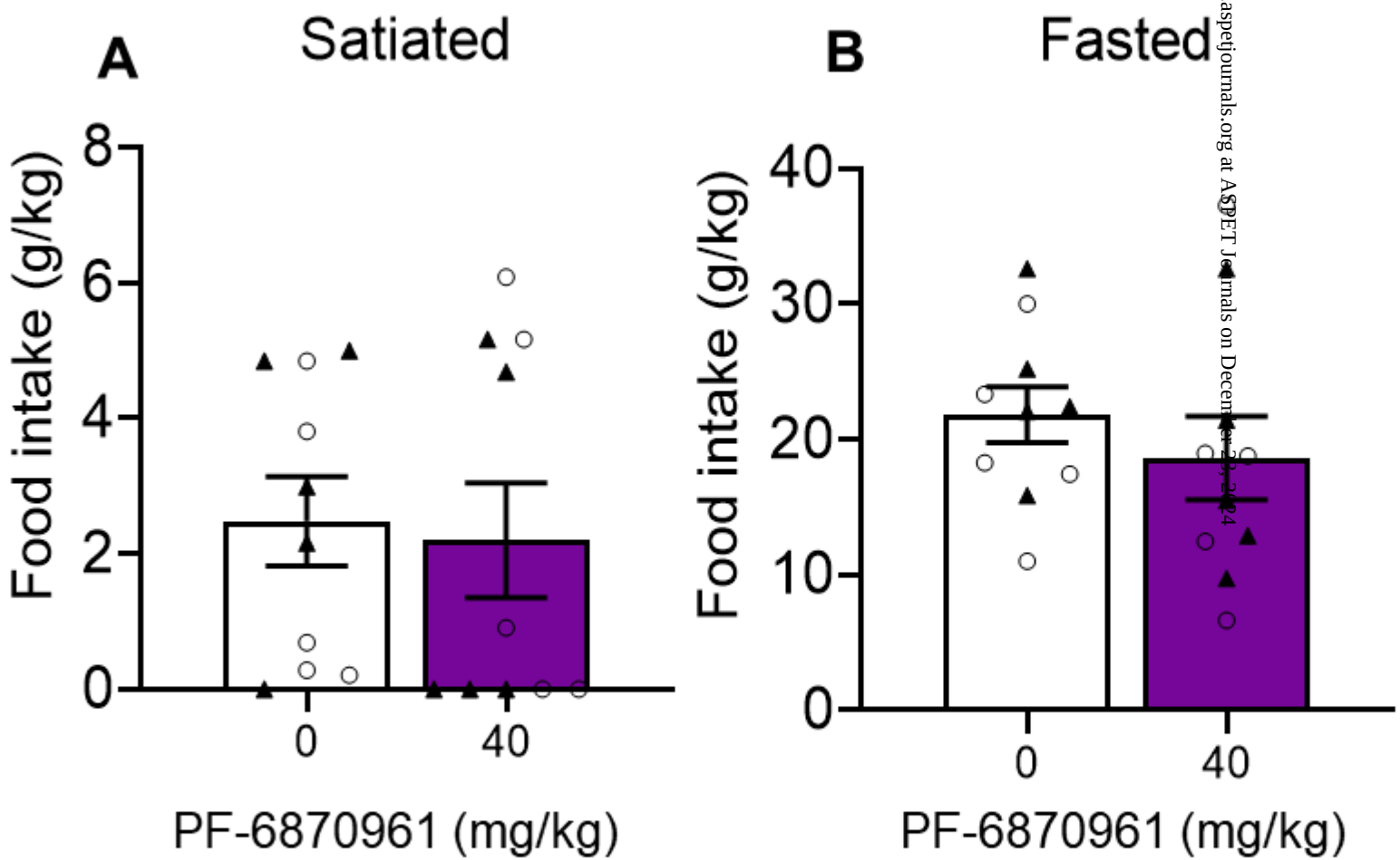

Figure 6

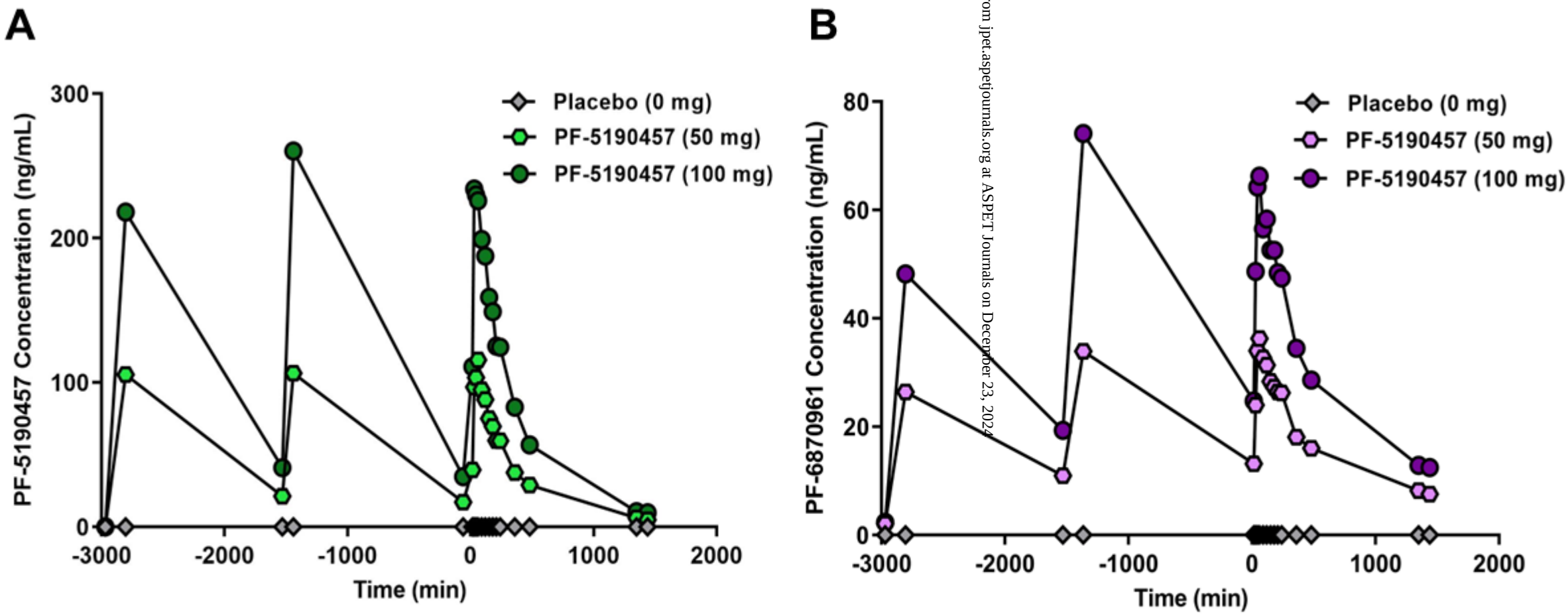

Figure 7